Received: 01 December 2021 | Revised: 08 January 2022 | Accepted: 27 January 2022
DOI: 10.22034/ecc.2022.317547.1274
Eurasian Chemical Communications
SAMI

FULL PAPER

Equilibrium and kinetic modeling studies for the adsorption-desorption of methyl violet 10B onto leather waste

Noor Hussein AL-Shammari* | **Dunya Edan AL-Mammar**

Department of Chemistry, College of Science, University of Baghdad, Baghdad, Iraq

***Corresponding Author:**
Noor Hussein AL-Shammari
Email: noor33hussien@gmail.com
Tel.: +07513194353

In this study, vegetable tanned leather waste of cow (VTLW-C) is used as adsorbent for removing methyl violet 10B dye from aqueous solution. The VTLW-C adsorbent was characterized by FTIR and SEM in order to evaluate its surface properties before using in adsorption experiments. Batch adsorption method was applied to study the effect of different factors such as weight of leather waste, time of shaking, and starting concentration of methyl violet 10B dye. Different isothermal models such as Langmuir, Freundlich, Temkin and Dubinin-Radushkevich (D–R) were used to analyze the experimental data. Kinetic study proceeds using (PFO) kinetic model and (PSO) kinetic model. The results showed better agreement with the Freundlich model; this means that the adsorption process was performed on a heterogeneous surface, and the maximum adsorption amounts of VTLW-C is 29.411 mg/g. From the value mean, free energy (E) for D–R isotherm the adsorption followed a physisorption nature process. Thermodynamic study proved that the adsorption process is exothermic and spontaneous. Experimental kinetic results are compatible with (PSO) model with correlation coefficients $R^2 > 0.9998$. Finally, the desorption and regeneration showed that the adsorbent could be easily reused related to the weak vanderwasll's force that accompanied the physical adsorption. VTLW-C is used as a good and low cost adsorbent to remove dye from wastewaters.

KEYWORDS

Adsorption; leather waste; methyl violet 10B; batch adsorption; thermodynamic; kinetic; desorption.

Introduction

The textile industry is one of the most important industries in the developing countries of the global economy, and is considered as a contributor to environmental pollution and health risks, because the wastewater of this industry contains a variety of pollutants from toxic metals, dissolved solids and residual dyes that pose threats to the water system and human and animal health [1]. Dyes are chemicals that appear in the effluents of the textile industries, so they are strictly removed due to their complex composition and synthetic origins [2]. To remove these different dyes from wastewater, many methods are used, the most important of which are flocculation, nano filtration, ozone, reverse osmosis, electrochemical and biological decomposition, photolysis, chemical oxidation, and adsorption [3,4]. Adsorption is one of the most powerful methods for removing dyes from their aqueous solutions due to its efficiency, high speed, low cost, flexibility and simplicity. Adsorption techniques have been successful in reducing

the concentration of dye from industrial effluents by using adsorbent materials such as polymeric materials [5], activated carbon, clay [6], chitin, peat, leather [7] and others. Adsorption process means the retention of ions, molecules or atoms on the surfaces of solid materials through physical or chemical bonding. Cationic dyes are widely used in industry and the most dangerous type of dye. It is reported that 12% of the annual production of cationic dyes is lost through industrial waterways that pollute the environment [8].

Methyl violet 10B (MV-10B) is a synthetic cationic dye also known as gentian violet, basic violet 3, and it belongs to the triarylmethane group. Its IUPAC name is: [4-[bis [4-(dimethylamino) phenyl] methylidene] cyclohexa-2,5-dien-1-ylidene]-dimethylazanium;chloride. Figure 1 shows the chemical formula for MV10B dye. This dye is widely used in the textile industries for dyeing cotton, wool, silk and nylon, in the manufacture of printing inks as well as biological stains, and is a dermatological agent in veterinary medicine. It is soluble in water and alcohol, and its C.I. number is 42555 [9].

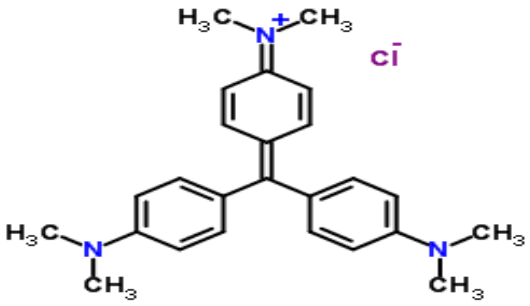

FIGURE 1 The chemical formula for MV-10B dye

In this work, the vegetable tanned leather waste of cow (VTLW-C) was used as a low cost adsorbent to remove (MV-10B) dye from its aqueous solutions. The properties of the adsorbent were evaluated using FTIR and SEM. To evaluate the properties of the adsorption process, batch adsorption experiments were conducted. Different isothermal models were studied and thermodynamic parameters were calculated for the adsorption process. Adsorption kinetic carried out using first-order pseudo and the second-order pseudo models to estimate the rat constants for the adsorption of MV-10B dye onto VTLW-C.

Materials

Adsorbent: Leather waste sample were obtained from a local tannery, which was supplied by Al-Wafa Leather Tannery Company (Baghdad city). The waste leather sample was cut into small pieces, and then initially stirred with distilled water for two hours to remove the excess tannin given the potential form absorbent interference in UV spectrophotometer. It was dried in an oven at 50 °C. The shrinkage temperature of vegetable tanned hides is between 75-85 °C in the humid state. The drying process of the leather sample is continued until it reaches a constant weight. Leather waste pieces are ground into granules using a laboratory mill into 7-14 mesh size particles. The samples are stored in desiccator to keep it dry in order to use these sample as adsorbent in our experiments after characterization of these sample using different technique (FTIR and SEM) to study surface properties.

Adsorbate: A stock solution related to (MV-10B) dye of 1000 mg/L was prepared by dissolution of dye (1 g) into distilled water (1000 mL). The stock solution was diluted to prepare a different concentration of (MV-10B) dye (5,15,25,35 and 45) mg/L.

Batch adsorption experiment: Batch adsorption experiments were performed to study the optimal state of adsorption of dye (MV-10B) on leather waste (VTLW-C) as an adsorbent at 298 K, using an electrostatic shaker at 150 rpm. The effect of cutaneous residue dose was studied by changing the weight (VTLW-C) from 0.05 g to 0.3 g at a dye concentration of 25 mg/L, and solution volume 25 mL, for 45 minutes. The effect of the shaking time was studied by taking different times from 5 to 90 minutes with an adsorbent weight of 0.2 g/50 mL of dye solution and a concentration of 25 mg/L. To study the effect of MV-10B dye concentrations, different concentrations from 5 mg/L to 45 mg/L with a weight of 0.1 g/25 mL of MV-10B dye were prepared for 45 minutes. The concentration of residual MV-10B dye was determined by a UV-Vis-Spectrophotometer (Shimadzu UV 1800, Japan). The removal efficiency R% and amount of adsorbed dye at equilibrium (mg/g) for the leather waste were calculated by the following equation [10]:

$$q_e = \frac{c_i - c_e}{m} \times v \qquad (1)$$

Removal efficiency

$$R\% = \frac{c_i - c_e}{c_i} \times 100 \qquad (2)$$

Where c_i and c_e are the concentration of MV-10B dye at starting and at the equilibrium (mg/L), m is the weight of leather waste (VTLW-C) (g) and V is the volume of the solution (L).

Isotherm models

Langmuir adsorption isotherm: In aqueous solution Langmuir equation written as [11]:

$$\frac{C_e}{Q_e} = \frac{1}{K_L\, Q_m} + \frac{1}{Q_m}.\, C_e \qquad (3)$$

Which: C_e is adsorbate's equilibrium concentration (mg/L), Q_e is the amount of the material adsorbed per gram of the adsorbent at equilibrium ($mg.g^{-1}$), Q_m is the maximum capacity of the mono-layer coverage (mg/g) and K_L is Langmuir isotherm constant ($L.mg^{-1}$). The values of Q_m and K_L are calculated from the slope as well as intercept of the line obtained when drawing C_e/Q_e versus C_e. The fundamental property can also be expressed by Langmuir's equation in terms of a separation factor R_s or dimensionless constant, using the following equation:

$$R_s = 1/\,(1 + K_L\, C_i) \qquad (4)$$

Where C_i is the starting concentration ($mg.\,L^{-1}$) and K_L Langmuir constant (L/mg).

The values R_s between 0 and 1 indicate that the adsorption is adequate, favorable ($0 < R_s < 1$), linear ($R_s = 1$), unfavorable ($R_s > 1$) and Irreversible ($R_s = 0$).

Freundlich adsorption isotherm: The Freundlich isotherm linear equation is expressed as [12]:

$$\ln q_e = \ln K_{Fr} + \left(\frac{1}{n_f}\right) \ln C_e \qquad (5)$$

Where C_e is the concentration at equilibrium (mg/L), K_{Fr} is Freundlich constant in ($mg.g^{-1}(mg.\,L^{-1})^{-1/n}$) related to adsorption capacity and n_f is the heterogeneity factor. The values of K_{Fr} and $1/n_f$ are calculated from the intercept and the slope of the linear relationship between $\ln q_e$ against $\ln C_e$. The adsorption curve is linear when it ($1/n_f = 1$) indicating that there is no interaction between the adsorbed types and the adsorption sites are of the homogeneous type [13]. While ($1/n_f < 1$), it indicates a favorable or normal adsorption, when the value of ($1/n_f > 1$), indicates cooperative adsorption [14].

Temkin isotherm: The linear relationship of the Temkin isotherm is described by the following equation:

$$q_e = B_T \ln A_T + B_T \ln C_e \qquad (6)$$

The values of A_T and B_T can be calculated from the intercept and the slope when plotting q_e

against $\ln C_e$ [11]. B_T which was calculated from the following equation:

$$B_T = RT/b_T \quad (7)$$

Which: b_T is Temkin isotherm constant, T is absolute temperature (K) and R is the gas constant (8.314 J/mol.K).

Dubinin-Radushkevich (D-R) isotherm: The linear D-R equation was obtained by the following way:

$$\ln q_e = \ln K_{D-R} - B\varepsilon^2 \quad (8)$$

Which: q_e is the amount of adsorbate in the adsorbent at equilibrium ($mg.g^{-1}$), K_{D-R} is theoretical adsorption saturation capacity ($mg.g^{-1}$), B is D-R isotherm constant ($mol^2.kJ^2$) and ε is Polanyi potential which described as [14]:

$$\varepsilon = R\,T\ln[1+\frac{1}{C_e}] \quad (9)$$

Which: R is the gas constant (8.314 J/mol.K), C_e is equilibrium concentration of adsorbate (mg/L) and T is the absolute temperature (K).

K_{D-R} and B values of the intercept and slope can be calculated from equation (1.15) when plotting $\ln q_e$ versus ε^2. The adsorption means free energy (E), which is calculated from the following equation:

$$E=\frac{1}{(2B)^{0.5}} \quad (10)$$

When the E value < 8kJ/mol the adsorption process can be classified as physical adsorption, while if the E value is in the range of 8kJ/mol to 16kJ/mol, then the adsorption process is a chemical adsorption process [15].

Adsorption thermodynamics:

Thermodynamic parameters such as standard gibbs free energy (ΔG°), standard enthalpy change (ΔH°), and standard entropy change (ΔS°) are important to check the spontaneity and randomness of the adsorption process. These parameters can be calculated by the following equations [16]:

$$\Delta G^\circ = -RT\ln K_{eq} \quad (11)$$

$$K_{eq} = \frac{C_i - C_e}{C_e}\ [V/m] \quad (12)$$

$$\Delta G^\circ = \Delta H^\circ - T\Delta S^\circ \quad (13)$$

Where R is the gas constant (8.314 J/mol.K), K_{eq} is the equilibrium constant of the adsorption, T is the absolute temperature (K), C_i is the starting concentration (mg/L) of the adsorbate, C_e is the equilibrium concentration (mg/L) of the adsorbate, V the volume of the adsorbate solution (L) and m is the weight of the adsorbent (g). The values of the standard entropy change ΔS° and standard enthalpy change ΔH° can be obtained from the intercept and slope of the linear plot of $\ln K_{eq}$ against 1/T through to the Van't Hoff equation [17]:

$$\ln K_{eq} = \frac{\Delta S^\circ}{R} - \frac{\Delta H^\circ}{RT} \quad (14)$$

Kinetic models

Pseudo-first-order (PFO) model or called Lagergren equation for liquid/solid adsorption systems based on solid capacitance has been widely used to describe adsorption kinetics [18,19]. It was expressed as [20]:

$$\ln (q_e - q_t) = \ln q_e - k_1.t \quad (15)$$

Pseudo-second-order (PSO) model of adsorption kinetics is described as [21]:

$$\frac{t}{q_t} = \frac{1}{k_2\, q_e^2} + \frac{t}{q_e} \quad (16)$$

Which q_e is equilibrium adsorption capacity (mg.), q_t is the adsorbed amount of adsorbate onto adsorbent at time t (mg.) and k_1 is rate constant for the adsorption process per min (min^{-1}) for the (PFO) model. k_2 is the equilibrium rate constant for a (PSO) model (g/mg.min). The slop and intercept of linear plots of $\ln (q_e - q_t)$ against t and t/q_t against t were applied to estimate the values of k_1 , q_e for the pseudo- first -order and k_2 and q_e for pseudo-second-order.

Results and discussion

Adsorbent characterization

FTIR spectra and SEM analysis of the VTLW-C: FTIR spectra was measured using Shimadzu IR-Affinity-1 Japan, scanned over a wavelength range from 450 to 4000. Figure 2 shows the FTIR spectra for VTLW-C. The peaks of (3500 to 3300) represent the symmetric stretching vibration of the OH group that overlaps with the vibration of the NH group for the adsorbent [22]. While the band intensity was about 2958 for VTLW-C from the C-H stretching vibration characteristics of the aliphatic parts [23], as for the peak at 1647 for the C = O carbonyl group and peak at 1541for the N-H group, clarifying the structure of the protein material for VTLW-C. The peak at 1238 is represented by a combination of bending N-H and stretching C-N [24]. Peaks in the range (1200-1000) represent the carbonyl group, amide group and aromatic aldehyde, while the peaks in the range (700-600) represent the functional group of aliphatic aldehyde (- NH wagging) [25].

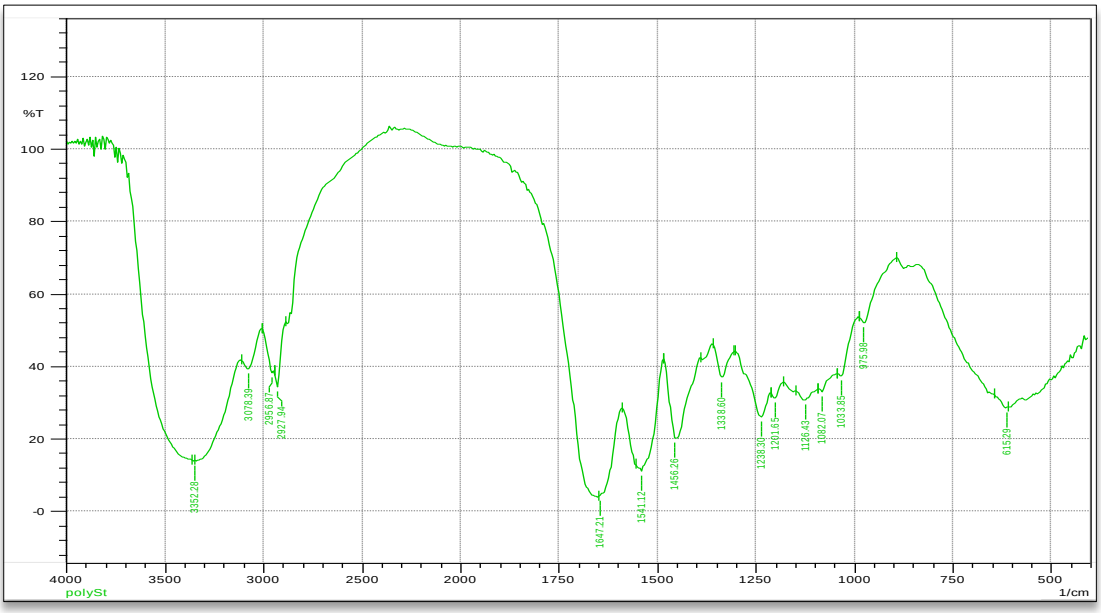

FIGURE 2 FTIR spectrophotometer analysis for VTLW-C.

SEM analysis was carried out using JTYS-1000, China. Figure 3 shows the SEM images of VTLW-C sample surface. SEM was considered as a good technique to estimate the shape surface, morphology and structure of solids. Figure 3 shows that the surface of the VTLW-C sample is mostly fiber-like and rod-like shapes. These resulting micrographs reveals that the adsorbent is in the form of fibers with its highly organized structure [26,27]. The collagen structure is preserved during tanning to ensure the stability of the leather waste [28].

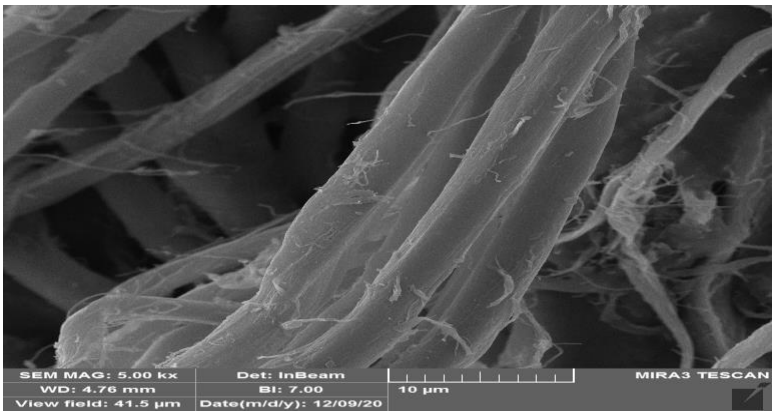

FIGURE 3 SEM images of VTLW-C sample surface

Effect of adsorbent amount:

The impact of VTLW-C amount on the removal percentage was evaluated at 298K. From Figure 4, we notice that the R% values increase with increasing amount of VTLW-C and reach nearly a constant value from 0.15 g to 0.3 g adsorbent. This increases could be attributed to the introduction of several active sites for adsorption [29]. The optimum weight chosen for all experiments is 0.1 g.

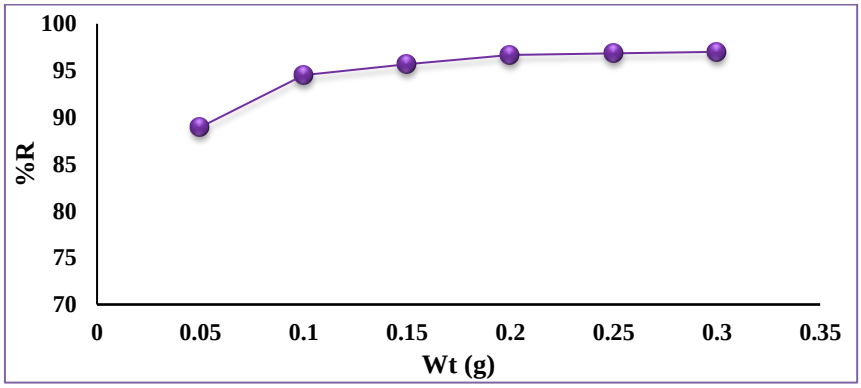

FIGURE 4 Impact of the leather amount on the removal percentage of MV-10B dye

Effect of shaking time: Figure 5 shows the impact of adsorption time on the adsorption of MV-10B dye. It turns out that the removal percentage increases in a time of 5 minutes and then reaches a stable state in a time of 45 minutes and remains stable. Therefore, 45 minutes were chosen as the best time for the adsorption experiments.

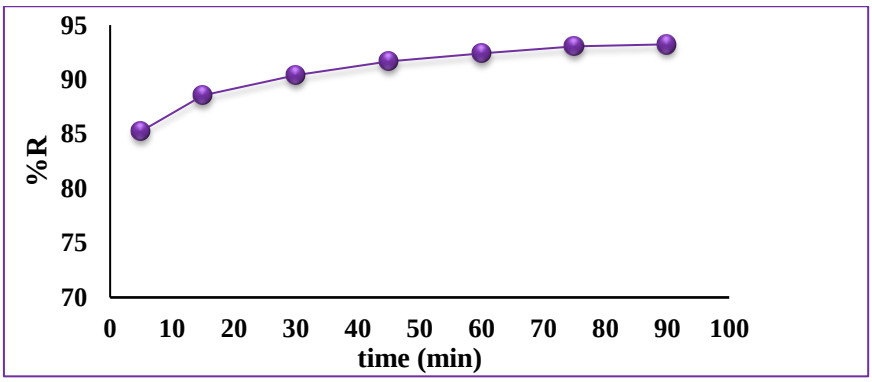

FIGURE 5 Impact of adsorption time on the removal percentage of MV-10B dye

Effect of starting MV-10B dye concentrations: Figure 6a shows the impact of starting concentration of MV-10B dye on to the removal percentage. In this Figure, the removal percentage decreases as the R% values change from 96.2% to 84.8% for VTLW-C, when the starting concentration of MV-10B dye is increased from 5 to 45 mg/L. This trend is due to the saturation of the adsorption sites on the surface of the adsorbent material and the lower adsorption [30]. Also, Figure 6b shows that the adsorption capacity changes from (1.2025 mg/g) to (9.8854mg/g) for VTLW-C. Therefore, 15 mg/L was selected as the optimal concentration for all experiments.

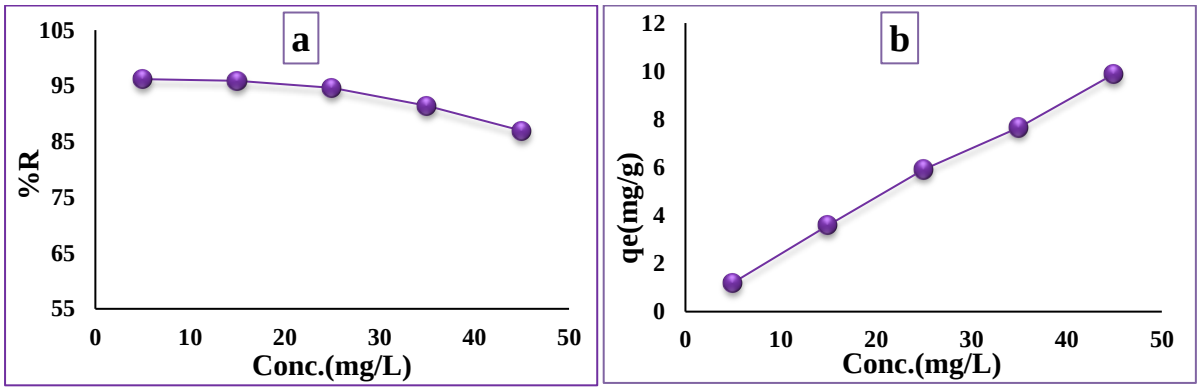

FIGURE 6 The influence of starting MV-10B dye concentration onto VTLW-C. Versus a-Removal Percentage R%, b- Amount of adsorbate adsorbed at equilibrium

Adsorption isotherms

Langmuir adsorption isotherm: Figure 7 shows the Langmuir isotherm for the adsorption of MV-10B dye onto VTLW-C at different temperatures. Table 1 represents the values of Langmuir constants, correlation coefficients and the separation factor.

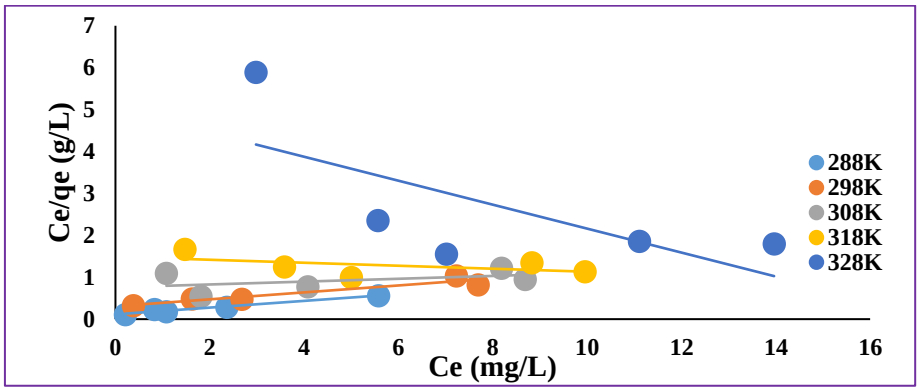

FIGURE 7 Langmuir isotherms for the adsorption of MV-10B dye onto VTLW-C at different temperatures

TABLE 1 Langmuir constants and R_s values at C_i equals to 45 mg/L for adsorption of MV-10B dye onto VTLW-C, at different temperatures

Temperature (K)	($mg.g^{-1}$)	(L/mg)	R^2	R_s
288	12.484	0.6941	0.9694	0.0310
298	12.091	0.2688	0.8914	0.0763
308	29.411	0.0447	0.2038	0.3318
318	28.089	0.0239	0.2498	0.4816
328	3.4989	0.0569	0.4800	0.2806

From this Table, the values $R^2$of lies between 0.2038 and 0.9694 were found. This indicates that the Langmuir isothermal model is not suitable, and the values of separation factor R_s for the adsorption of 45 mg/L MV-10B dye onto leather sample at different temperatures is $0<R_s<1$, indicated that the adsorption process is favorable [31].

Freundlich isotherm model: Figure 8 shows the Freundlich isotherm of MV-10B dye onto VTLW-C, at different temperatures. Table 2 shows the experimental Freundlich isotherm parameters for the adsorption of MV-10B dye onto leather waste sample.

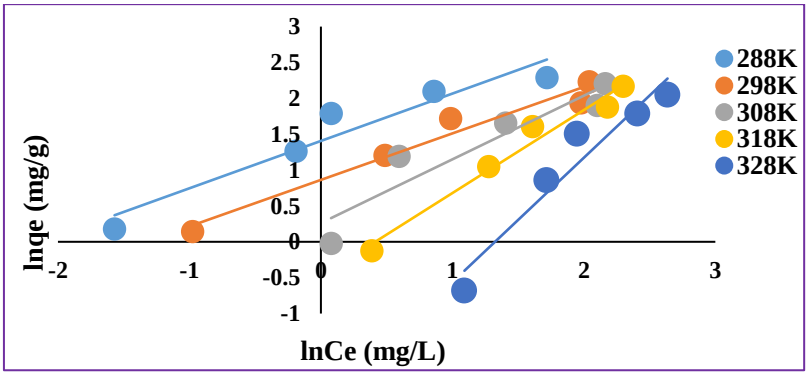

FIGURE 8 Freundlich isotherm plots for the adsorption of MV-10B dye adsorption onto VTLW-C at different temperatures

TABLE 2 The values of Freundlich isotherm constants for the adsorption of MV-10B dye onto VTLW-C at different temperatures

Temperature (K)	Slope $(1/n_f)$	n_f	Intercept	K_{Fr} $(mg.g^{-1}(mg.L^{-1})^{-1/n})$	R^2
288	0.6600	1.5151	1.4060	4.0796	0.9209
298	0.6481	1.5429	0.8628	2.3697	0.9628
308	0.8876	1.1266	0.2616	1.2990	0.8816
318	1.1578	0.8637	-0.4786	0.6196	0.9729
328	1.7341	0.5766	-2.2962	0.1006	0.9274

In this Table, the values of R^2lies between 0.8816- 0.9729. These values are reasonable with Freundlich model isotherm than Langmuir isotherm. The values $(1/n_f)$ range between (0 and 1) which gives a measure of the intensity of adsorption and surface heterogeneity [32]. This means that the adsorption process was performed on a heterogeneous surface.

Temkin isotherm model: Figure 9 shows Temkin adsorption isotherm plots for the adsorption of MV-10B dye onto VTLW-C at different temperatures. Table 3 shows the Temkin isotherm for this process.

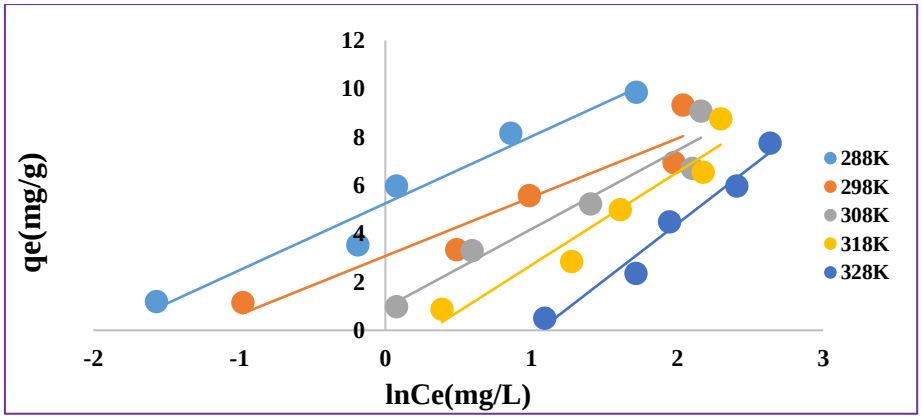

FIGURE 9 Temkin isotherm plots for MV-10B dye adsorption onto VTLW-C at different temperatures

TABLE 3 Temkin isotherm constants for the adsorption of MV-10B dye onto VTLW-C at different temperatures

Temperature (K)	B_T (J.mol^{-1})	b_T	Intercept	A_T (L/g)	R^2
288	2.7675	865.19	5.2514	6.6693	0.9575
298	2.4310	1019.1	3.0735	3.5405	0.9097
308	3.2586	785.83	0.9258	1.3285	0.9308
318	3.8421	688.12	-1.1483	0.7416	0.9280
328	4.6581	585.43	-4.9121	0.3483	0.9693

In this Table, increasing temperature leads to decrease in the values of A_T indicating that the adsorption process is an exothermic [33]. The small value of B_T <8 KJ.mol^{-1} indicates a weak interaction between the MV-10B ions and VTLW-C surface, indicating that the adsorption is most likely physisorption [34,35].

Dubinin–Radushkevich (D-R) isotherm: Figure 10 shows the D-R isotherm plots for the adsorption of MV-10B dye onto VTLW-C at different temperatures. Table 4 shows the D-R isotherm constants for this process.

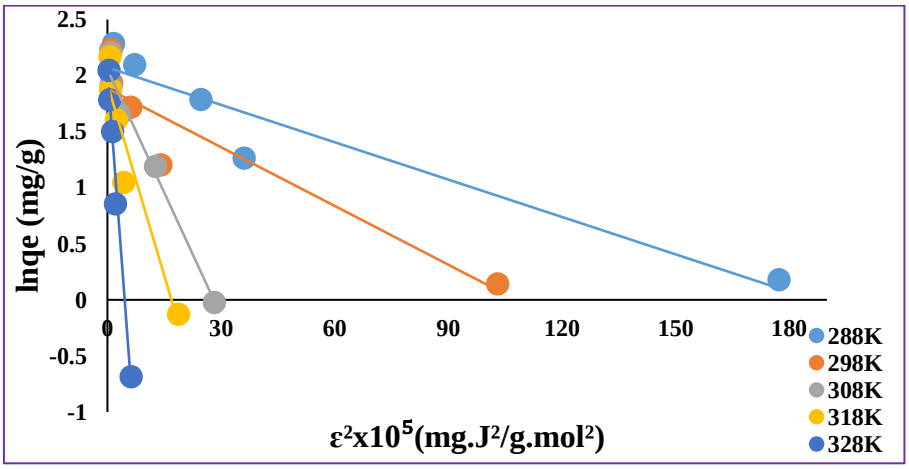

FIGURE 10 D-R isotherm for the adsorption of MV-10B dye onto VTLW-C at different temperatures

TABLE 4 D-R isotherms constants for the adsorption of MV-10B dye onto VTLW-C at different temperatures

Temperature (K)	B ($Mol^2.KJ^2$)	E (kJ/mol)	K_{D-R} (mg/g)	R^2
288	0.0111	6.7115	7.9422	0.9168
298	0.0175	5.3452	6.5909	0.8766
308	0.0732	2.6135	7.8123	0.9722
318	0.1138	2.0961	6.8544	0.9183
328	0.4491	1.0551	7.7299	0.9769

From Table 4, it is revealed that mean free energy (E) values were less than (8kJ/mol) which suggested that the adsorption of MV-10B dye onto VTLW-C sample is of physisorption process [14].

Adsorption thermodynamics: Figure 11 refers to the Van't Hoff plots for the adsorption of MV-10B dye onto VTLW-C. Table 5 shows thermodynamic parameters ΔG°, ΔS° and ΔH° for the adsorption of MV-10B dye onto leather waste at different temperatures.

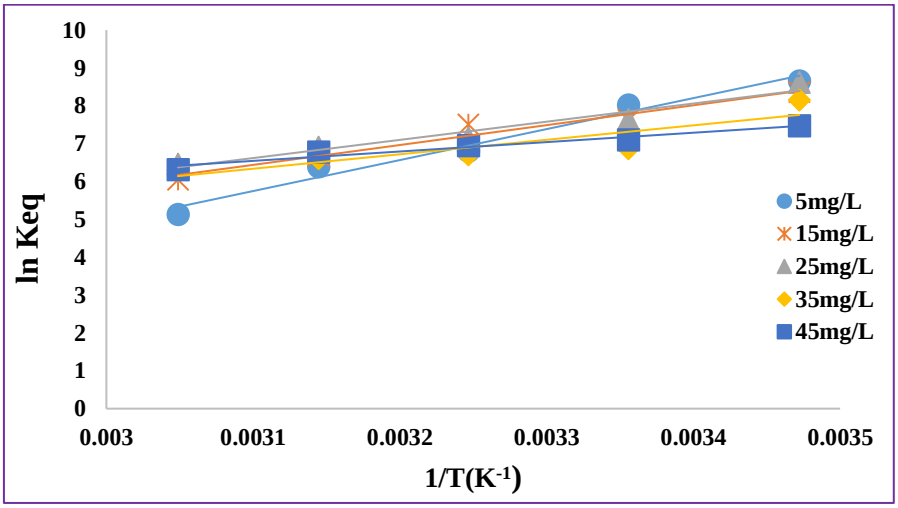

FIGURE 11 Van't Hoff plots for the adsorption of MV-10B dye onto VTLW-C at different temperatures

TABLE 5 Thermodynamic parameters for the adsorption of MV-10B dye onto VTLW-C at different temperatures

c_i (mg/L)	(-) ΔH^o (kJ/mol)	(-) ΔS^o (kJ/mol)	(-) ΔG^o(kJ/mol) 288K	298K	308K	318K	328K
5	68.0218	0.16307	20.7306	19.8904	17.4394	16.9039	13.9991
15	43.6210	0.08169	20.0240	18.8959	19.2223	17.6612	16.4952
25	39.9304	0.06875	20.6377	18.9277	18.3276	18.2602	17.6241
35	31.7644	0.04578	19.5105	17.0154	17.1784	17.4704	17.1454
45	20.6187	0.00950	17.9016	17.5925	17.8007	17.9253	17.2350

In this table, the negative values of ΔG° show that the adsorption process is favourable and spontaneous at decreasing temperatures, and no external energy needs to be introduced from outside the system [36]. The negative values of ΔH° indicate that the adsorption of MV-10B dye onto VTLW-C occurs with releasing heat and exothermic process. The negative values of ΔS° indicated that dye in the solid phase is arranged in an orderly manner, where adsorption causes a decrease disorder in system [22].

Kinetic study: The pseudo-first-order (PFO) and pseudo-second-order (PSO) were used to study the mechanisms of adsorption of MV-10B dye onto the leather waste sample as adsorbent to find the appropriate kinetic model for this process. Kinetic experiments were performed at starting concentration of MV-10B dye (5, 15, 25, 35 and 45) mg/L, adsorbent dosage 0.2g/50mL and at different temperatures in the range of 288 to 328 K.

Pseudo-First-Order (PFO) Model: The values k_1 and ($q_{e\ cal}$) can be estimated from the slope and the intercept of plots, $\ln(q_e - q_t)$ versus t, of Figure 12. Table 6 shows the kinetic constants for this model.

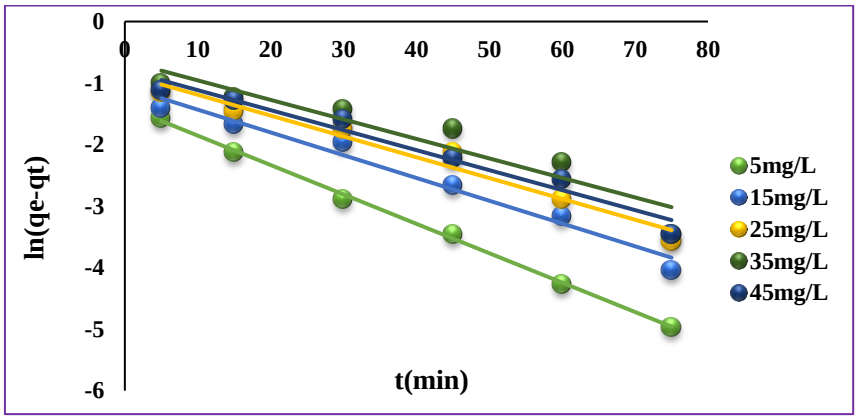

FIGURE 12 Pseudo-first-order kinetic plot for the adsorption of MV-10B dye onto VTLW-C at 298K

TABLE 6 Pseudo-first-order kinetic parameters of the adsorption of MV-10B dye onto VTLW-C at 298K

C_i (mg/L)	$q_{e\ exp}$ (mg/g)	$q_{e\ cal}$ (mg/g)	k_1 (min^{-1})	R^2
5	1.2049	0.2524	0.0478	0.9984
15	3.5116	0.3456	0.0370	0.9741
25	5.7549	0.4263	0.0338	0.9684
35	7.2211	0.5275	0.0317	0.8886
45	9.5031	0.4536	0.0325	0.9636

Table 6 displays the highest value of $R^2$is 0.9984 and the lowest value of R^2 is 0.8886. Also, for all MV-10B dye concentration and at 298K, the calculated values of equilibrium adsorption capacity ($q_{e\ cal}$)differ from the experimental ($q_{e\ exp}$) values. This means that the (PFO) kinetic model is adequately not applicable.

Pseudo-second-order(PSO) Model: The values of $q_{e\ cal}$ and k_2 are calculated from the slope and the intercept of the plot between t/q_tversus t, as shown in Figure 13. Table 7 summarizes the corresponding model parameters, with values of the correlation coefficient at 298K.

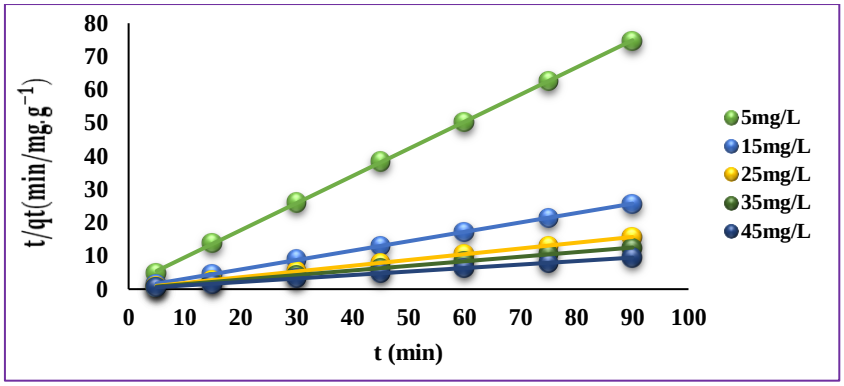

FIGURE 13 Pseudo-second-order kinetic plot for adsorption of MV-10B dye onto VTLW-C at 298K

TABLE 7 Pseudo-second-order kinetic parameters of the adsorption of MV-10B dye onto VTLW-C at 298K

C_i (mg/L)	$q_{e\ exp}$ (mg/g)	$q_{e\ cal}$ (mg/g)	k_2 (g/mg.min)	R^2
5	1.2049	1.2245	0.4828	0.9999
15	3.5116	3.5360	0.2925	0.9999
25	5.7549	5.7836	0.2264	0.9999
35	7.2211	7.2516	0.1702	0.9998
45	9.5031	9.5328	0.2088	1.0000

It was noticed from this table that values of R^2 lie between (0.9998 and 1.0000); also, these values are higher than that for (PFO) kinetic model. Moreover, the values of q_e calculated ($q_{e\ cal}$) agree with the values of q_e experimental ($q_{e\ exp}$). These obtained results indicated that the adsorption of MV-10B dye onto leather waste sample is more representable by Pseudo-second-order(PSO) kinetic model.

Desorption: The regeneration of VTLW-C adsorbent loaded with MV-10B dye was carried out at a concentration of 15mg/L and 0.1g leather waste weight. Ethanol at a concentration of 75% was used for this adsorption process volume of 25 mL in 100 mL conical flasks with a time taken 4 hours and a shaking speed of 150rpm at 298K that occurs during three cycles. Figure 14 shows desorption of MV-10B dye from VTLW-C surface at 298K.

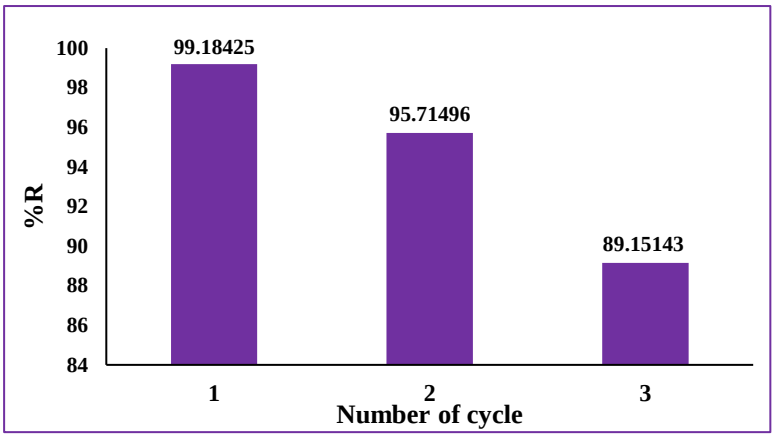

FIGURE 14 Desorption of MV-10B dye from VTLW-C surface at 298K

In this figure, we notice that the removal percentage decreases from 99.1% to 89.1%. This decrease in the adsorption of MV-10B dye from the surface of leather waste is due to the possibility of a large adsorption energy due to the multiple contact points between the adsorbent material and the large dye molecules [37].

It was clear that these adsorbents can be repeatedly renewed and reused in the process of removing dyes from wastewater. The high desorption removal percent mainly indicates that the adsorption of the MV-10B dye onto the VTLW-C surface is a physisorption type, with weak vander waal's forces conjugated between the adsorbent surface and the molecules of dye.

Conclusion

From this research, we can conclude that VTLW-C was a promise material removal MV-10B dye from aqueous solution. The adsorbent was characterized by FTIR and SEM analysis shows that the surface of VTLW-C sample is mostly fiber-like and rod-like shapes. Studying the optimum conditions for the adsorption process predicted that the best amount of VTLW-C is 0.1 g with 15 mg/L starting concentration dye and for 45 min as adsorption time. Among different adsorption isotherm models used, Freundlich model is better suited the experimental data. From the value E (mean free energy) that calculated form Dubinin–Radushkevich isotherm, we have estimated that the adsorption of MV-10B dye is physisorption type. Thermodynamic study indicated that the adsorption process occurs spontaneous with releasing heat. Kinetic results are compatible with Pseudo-second-order(PSO) model. Desorption process for the MV-10B dye from the VTLW-C surface occurs easily due to the weak vander waal's force that accompanied the physical adsorption.

Acknowledgements

The authors thank everyone who helped to complete this research.

Orcid:

Noor Hussein AL-Shammari:
https://orcid.org/0000-0002-4062-6628

References

[1] R. Kishor, D. Purchase, G.D. Saratale, L.F.R. Ferreira, M. Bilal, H.M.N. Iqbal, R.N. Bharagava, *Environ. Technol. Innov.*, **2021**, *22*, 101425. [crossref], [Google Scholar], [Publisher]

[2]G. Crini, G. Torri, E. Lichtfouse, G.Z. Kyzas, L.D. Wilson, N Morin-Crini, *Environ. Chem. Lett.*, **2019**, *17*, 1645–1666. [crossref], [Google Scholar], [Publisher]

[3] S. Shakoor, A. Nasar, *Groundw. Sustain. Dev.*, **2018**, *7*, 30–38. [crossref], [Google Scholar], [Publisher]

[4] Y.H. Wu, K. Xue, Q.L. Ma, T. Ma, Y.L. Ma, Y.G. Sun, W.X. Ji, *Microporous Mesoporous Mater.*, **2021**, *312*, 110742. [crossref], [Google Scholar], [Publisher]

[5] Z. Zhao, C. Bai, L. An, X. Zhang, F. Wang, Y. Huang, M. Qu, Y. Yu, *J. Environ. Chem. Eng.*, **2021**, *9*, 104797. [crossref], [Google Scholar], [Publisher]

[6] L.C. Oliveira, R.V.R. Rios, J.D. Fabris, K. Sapag, V.K. Garg, R.M. Lago, *Appl. Clay Sci.*, **2003**, *22*, 169–177. [crossref], [Google Scholar], [Publisher]

[7] L.C.A. Oliveira, M. Gonçalves, D.Q.L. Oliveira, M.C. Guerreiro, L.R.G. Guilherme, R.M. Dallago, *J. Hazard. Mater.*, **2007**, *141*, 344–347. [crossref], [Google Scholar], [Publisher]

[8] R. Foroutan, S.J. Peighambardoust, S.H. Peighambardoust, M. Pateiro, J.M. Lorenzo, *Molecules*, **2021**, *26*, 2241. [crossref], [Google Scholar], [Publisher]

[9] M. Abbas, Z. Harrache, M. Trari, *Adsorp. Sci. Technol.*, **2019**, *37*, 566-589. [crossref], [Google Scholar], [Publisher]

[10] L. Xia, C. Li, S. Zhou, Z. Fu, Y. Wang, P. Lyu, J. Zhang, X. Liu, C. Zhang, W. Xu, *Polymers*,

2019, *11*, 1786. [crossref], [Google Scholar], [Publisher]
[11] F. Bouatay, S. Dridi, M. Mhenni., *Int. J. Environ. Res.*, **2014**, *8*, 1053-1066. [crossref], [Google Scholar], [Publisher]
[12] M.A. Atiya, M.J.M. Ridha, M.A. Saheb, *Iraqi J. Sci.*, **2020**, *61*, 2797-2811. [crossref], [Google Scholar], [Publisher]
[13] K. Allam, K. Gourai, A. El Bouari, B. Belhorma, L. Bih, *J. Mater. Environ. Sci.*, **2018**, *9*, 1750-1761. [crossref], [Google Scholar], [Publisher]
[14] A. Dada, A. Olalekan, A. Olatunya, O. Dada, *IOSR J. Appl. Chem.*, **2012**, *3*, 38-45. [crossref], [Google Scholar], [Publisher]
[15] F. Batool, J. Akbar, S. Iqbal, S. Noreen, S.N.A. Bukhari, *Bioinorg. Chem. Appl.*, **2018**, *2018*, Article ID 3463724. [crossref], [Google Scholar], [Publisher]
[16] S. Raghav, D. Kumar, *J. Chem. Eng. Data*, **2018**, *63*, 1682–1697. [crossref], [Google Scholar], [Publisher]
[17] E.C. Lima, A.A. Gomes, H.N. Tran, *J. Mol. Liq.*, **2020**, *311*, 113315. [crossref], [Google Scholar], [Publisher]
[18] S. Mashhadi, R. Sohrabi, H. Javadian, M. Ghasemi, I. Tyagi, S. Agarwal, V.K. Gupta, *J. Mol. Liq.*, **2016**, *215*, 144–153. [crossref], [Google Scholar], [Publisher]
[19] M.S. Miao, Q. Liu, L. Shu, Z. Wang, Y.Z. Liu, Q. Kong, *Process Saf. Environ. Prot.*, **2016**, *104*, 481–489. [crossref], [Google Scholar], [Publisher]
[20] G.W. Kajjumba, S. Emik, A. Öngen, H.K. Özcan, S. Aydın, *Modelling of Adsorption Kinetic Processes—Errors, Theory and Application*, Advanced Sorption Process Applications, **2019**, 1-19. [crossref], [Google Scholar], [Publisher]
[21] A.B. Wassie, V.C. Srivastava, *J. Environ. Chem. Eng.*, **2016**, *4*, 1117–1125. [crossref], [Google Scholar], [Publisher]
[22] J.S. Piccin, L.A. Feris, M. Cooper, M. Gutterres, *J. Chem. Eng. Data*, **2013**, *58*, 873–882. [crossref], [Google Scholar], [Publisher]
[23] C. Manera, A.P. Tonello, D. Perondi, M. Godinho, *Environ. Technol.*, **2018**, *40*, 2756-2768. [crossref], [Google Scholar], [Publisher]
[24] J. Anandkumar, B. Mandal, *J. Hazard. Mater.*, **2011**, *186*, 1088–1096. [crossref], [Google Scholar], [Publisher]
[25] M.E.S. Mirghani, H.M. Salleh, Y.B.C. Man, I. Jaswir, *Adv. in Nat. Appl. Sci.*, **2012**, *6*, 651-659. [Google Scholar], [Publisher]
[26] S. Tahiri, A. Messaoudi, A. Albizane, M. Azzi, M. Bouhria, S.A. Younssi, J. Bennazha, J. Mabrour, *Water Qual. Res. J.*, **2003**, *38*, 393–411. [crossref], [Google Scholar], [Publisher]
[27] D.Q.L. Oliveira, M. Gonçalves, L.C.A. Oliveira, L.R.G. Guilherme, *J. Hazard. Mater.*, **2008**, *151*, 280–284. [crossref], [Google Scholar], [Publisher]
[28] R.R. Gil, B. Ruiz, M.S. Lozano, M.J. Martín, E. Fuente, *Chem. Eng. J.*, **2014**, *245*, 80–88. [crossref], [Google Scholar], [Publisher]
[29] U. Itodo, M. Khan, D. Feka, B. Ogoh, *J Water Technol. Treat Meth.*, **2018**, *1*, 1-8. [crossref], [Google Scholar], [Publisher]
[30] E. Rápó, S. Tonk, *Molecules*, **2021**, *26*, 5419. [crossref], [Google Scholar], [Publisher]
[31] C. Clavijo, J.F. Osma., *Water*, **2019**, *11*, 1906. [crossref], [Google Scholar], [Publisher]
[32] F. Kallel, F. Bouaziz, F. Chaari, L. Belghith, R. Ghorbel, S.E. Chaabouni, *Process Saf. Environ. Prot.*, **2016**, *102*, 30–43. [crossref], [Google Scholar], [Publisher]
[33] A.M. Aljeboree, A.N. Alshirifi, A.F. Alkaim, *Arab. J. Chem.*, **2017**, *10*, S3381–S3393. [crossref], [Google Scholar], [Publisher]
[34] A.V. Borhade, A.S. Kale, *Appl. Water Sci.*, **2017**, *7*, 4255–4268. [crossref], [Google Scholar], [Publisher]
[35] S.H. Abbas, M.A. A.-K. Ahmed, W.H. Ali, *Journal of Engineering and Sustainable Development (JEASD)*, **2018**, *22*, 229–246. [crossref], [Google Scholar], [Publisher]
[36] G.L. Dotto, E.C. Lima, L.A.A. Pinto, *Bioresour. Technol.*, **2012**, *103*, 123–130. [crossref], [Google Scholar], [Publisher]

[37] A.A. Inyinbor, F.A. Adekola, G.A. Olatunji, *Water Resour. Ind.*, **2016**, *15*, 14–27. [crossref], [Google Scholar], [Publisher]

How to cite this article: Noor Hussein AL-Shammari*, Dunya Edan AL-Mammar. Equilibrium and kinetic modeling studies for the adsorption-desorption of methyl violet 10B onto leather waste**.** *Eurasian Chemical Communications*, 2022, 4(2), 175-189. **Link:** http://www.echemcom.com/article_143917.html